

THE RATIO OF THE COUPLING CONSTANTS IN BETA-DECAY

THE RATIO OF THE SCALAR AND TENSOR COUPLING
CONSTANTS IN BETA-DECAY

By
WOLFGANG ZERNIK, B.Sc.

A Thesis
Submitted to the Faculty of Arts and Science
in Partial Fulfilment of the Requirements
for the Degree
Master of Science

McMaster University

September 1956

(I)

McMASTER UNIVERSITY
LIBRARY
KINGSTON, ONTARIO

MASTER OF SCIENCE (1956)
(Physics)

McMASTER UNIVERSITY,
Hamilton, Ontario

TITLE: The Ratio of the Scalar and Tensor Coupling Constants
in Beta-Decay.

AUTHOR: Wolfgang Zernik, B.Sc. (Manchester University).

SUPERVISOR: Professor M. A. Preston.

NUMBER OF PAGES: \bar{V} , 43.

SCOPE AND CONTENTS:

The beta-decay interaction contains two terms which consist of invariant products of two scalars and two tensors respectively. The relative absolute magnitude of these two terms is fairly well established but there has been some controversy over their relative sign. In this thesis the form of the interaction is investigated by means of an analysis of the second-forbidden decay spectrum of Cs^{137} and it is concluded that the relative sign of the scalar and tensor terms is negative.

ACKNOWLEDGMENTS

The author wishes to express his gratitude to Professor M. A. Preston for suggesting this project and for his constant advice and encouragement throughout its execution.

TABLE OF CONTENTS.

INTRODUCTION.

CHAPTER I, Page 2.

The general theory of beta-decay.

CHAPTER II, Page 8.

The theory of forbidden spectra and the method
of conics.

CHAPTER III, Page 17.

Construction and analysis of the conics.

CONCLUSIONS.

LIST OF ILLUSTRATIONS.

- FIGURE 1. Page 29. Decay scheme of Cs¹³⁷.
- FIGURE 2. Page 30. Fermi-plot of the second-forbidden transition of Cs¹³⁷.
- FIGURE 3. Page 30a. Conics for $R_0 = R_0$.
- FIGURE 4. Page 30b. Conics for $R_0 = 0.8 R_0$.
- FIGURE 5. Page 30c. Conics for $R_0 = 0.5 R_0$.

INTRODUCTION.

This thesis deals with the resolution of one of the few remaining ambiguities in the theory of beta-decay.

It is known that the beta-decay interaction matrix element may be written as the sum of three terms:

$$H = g_s H_s + g_t H_t + g_p H_p \quad (1)$$

These terms represent the "scalar", "tensor" and "pseudoscalar" interactions respectively. There is at present no direct evidence for the last term and in any case its effect would generally be very small, consequently it will not be considered in detail in what follows.

The ratio $K^2 = g_t^2 / g_s^2$ can be calculated fairly simply from the experimental results; its value appears to lie between 1 and 2. However, the determination of the sign of g_t/g_s is considerably more difficult and calculations leading to both positive and negative values have been published.

This thesis describes an attempt to determine the sign of g_t/g_s by means of an analysis of the second forbidden decay of Cs^{137} . The results seem to show conclusively that g_t/g_s is negative.

The lay-out of the thesis is as follows:

Chapter 1 gives a brief outline of the general theory of beta-decay and a summary of the more recent results on the nature of the interaction.

Chapter 11 outlines the theory of forbidden spectra and explains the method of finding g_t/g_s by drawing conics. The details of the calculation and the analysis of the results are given in Chapter 111.

Chapter 1. The General Theory of Beta-Decay.

The following summary is merely intended to provide a general background for the material of Chapters II and III. More complete expositions may be found in several excellent review articles (1,2,3,4,5).

A basic assumption of the theory is that beta-decay is a process analogous to that of electromagnetic radiation. Therefore the transition probability per second should be given by the usual formula from first-order perturbation theory.

$$W = \frac{2\pi}{\hbar} |H|^2 \frac{dn}{dE} \quad (2)$$

$\frac{dn}{dE}$ is the energy density of the final states, i.e., the number of cells in phase space available to the electron and the neutrino:

$$\frac{dn}{dE} = \frac{p^2 dp d\omega_e q^2 d\omega_n}{(2\pi\hbar)^3 (2\pi\hbar)^3 c} \quad (3)$$

Where p, q are the momenta of electron and neutrino respectively and $d\omega_e, d\omega_n$ are the elements of solid angle.

We can put:

$$q = \frac{1}{c} (W_0 - W) \quad (4)$$

Where W_0 is the end-point energy of the spectrum and W the energy of the electron, and integrate over the solid angles assuming isotropic distribution, then we obtain:

$$\frac{dn}{dE} = (4\pi)^4 \hbar^6 c^3)^{-1} (W_0 - W)^2 p^2 dp \quad (5)$$

This is the famous statistical factor.

The integrand of the matrix element H must clearly contain the wave-functions of the four particles involved. As the simplest plausible expression we write:

$$H = g \int U_f^* Q U_i \psi^* \phi dV \quad (6)$$

Here g is a nucleon-lepton coupling constant which is the same for all beta-decays and must be evaluated by experiment. U_f and U_i are the final and initial nuclear wave-functions. ψ is the wave function of the electron, ϕ that of the neutrino; ψ, ϕ are normalised to unit volume. Q is a charge-exchange operator that converts a neutron into a proton. It is of modulus unity. The lepton wave-functions have to be evaluated at the co-ordinates of the nucleus and the entire expression integrated over the nuclear volume.

Since the neutrino, at least, is moving at relativistic velocities, the wave-functions in Equation 6 should be of the 4-component Dirac type. However, products of Dirac wave-functions like $(U_f^* U_i^* \psi^* \phi)$ are not relativistically invariant. In order to make products of this type that are invariant we have to include one or more of the Dirac matrices. In his famous article (6) Pauli has shown that from two Dirac wave-functions such as ψ^*, ϕ one can form only five bilinear expressions that transform in different ways under Lorentz transformations. These quantities transform like a scalar, a vector, a second-order tensor, a pseudovector and a pseudoscalar, respectively. Multiplying any one of these quantities by the corresponding quantity formed from U_f^*, U_i we obtain an invariant. Thus the integrand of Equation 6 could be an arbitrary linear combination of the following five forms:

(3)

$$\begin{aligned}
S \text{ Scalar} & : (U_f^* \beta U_1) (\psi^* \beta \phi) \\
V \text{ Vector} & : (U_f^* U_1) (\psi^* \phi) - (U_f^* \underline{\alpha} U_1) (\psi^* \underline{\alpha} \phi) \\
T \text{ Tensor} & : (U_f^* \beta \underline{\sigma} U_1) (\psi^* \beta \underline{\sigma} \phi) + (U_f^* \beta \underline{\alpha} U_1) (\psi^* \beta \underline{\alpha} \phi) \\
A \text{ Pseudovector} & : (U_f^* \underline{\sigma} U_1) (\psi^* \underline{\sigma} \phi) - (U_f^* \gamma_5 U_1) (\psi^* \gamma_5 \phi) \\
P \text{ Pseudoscalar} & : (U_f^* \beta \gamma_5 U_1) (\psi^* \beta \gamma_5 \phi)
\end{aligned}$$

Here, $\beta, \underline{\alpha}, \underline{\sigma}, \gamma_5$ are the usual symbols for certain combinations of 4×4 matrices that occur in the theory of the Dirac equation.

Attempts have been made to pick out particular combinations of these interactions on a priori theoretical grounds, but such combinations have not fitted the experimental results. At present it is thought that the correct combination contains roughly equal quantities of the scalar and tensor interactions and possibly some pseudoscalar interactions as well (7). Each interaction has associated with it its own selection rules. For allowed transitions they are as follows:

Scalar	$\Delta J = 0$, no
Tensor	$\Delta J = 0, \pm 1$	(except $0 \rightarrow 0$), no
Pseudoscalar	$\Delta J = 0$,	yes

Here, "no" means no parity change.

The distinction between allowed and forbidden spectra will be explained in Chapter 11. It is clear that the pseudoscalar interaction is forbidden when either the scalar or tensor interaction is allowed, so that

for the present we may neglect it.

We can calculate the lepton parts of these matrix elements by taking plane-wave solutions for the neutrino and Coulomb wave-functions belonging to continuous eigenvalues for the electron. Then we obtain:

$$|H|^2 = g^2 F_0(Z, W) [|\int 1|^2 + K^2 |\int \sigma|^2] \quad (7)$$

Where $\int 1$ and $\int \sigma$ represent the scalar and tensor nuclear matrix elements respectively. $F_0(Z, W)$ is a Coulomb correction factor given by:

$$F_0(Z, W) = \frac{2(2pR)^{2S-2} e^{\pi\alpha ZW/p} |\Gamma(S+1-\alpha ZW/p)|^2 (1+2S)}{[\Gamma(2S+1)]^2} \quad (8)$$

Here R is the nuclear radius; α the fine structure constant $\frac{1}{137}$; Z the nuclear charge to be taken negative for positron emitters; $S = (1 - \alpha^2 Z^2)^{\frac{1}{2}}$ and $F_0(Z, W)$ is exactly unity for $Z = 0$ and not far different from unity for charges as high as $Z = 20$. Combining Equations 2, 5 and 7 we finally obtain for the decay probability per second for an allowed transition:

$$Wdp = g^2 (2\pi^3 \hbar^7 c^3)^{-1} F_0(Z, W) (W_0 - W)^2 p^2 [|\int 1|^2 + K^2 |\int \sigma|^2] dp \quad (9)$$

Integrating this expression over the total energy range we obtain for the half-life t :

$$\ln 2/t = (2\pi^3)^{-1} mc^2/\hbar [mc^2 (\hbar/mc)^3]^{-2} \cdot f(Z, W) g^2 [|\int 1|^2 + K^2 |\int \sigma|^2] \quad (10)$$

where $f(Z, W)$ is a dimensionless function given by:

$$f(Z, W) = (mc^2)^{-5} \int_{mc^2}^{W_0} F_0(Z, W) (W_0 - W)^2 (W^2 - m^2 c^4)^{\frac{1}{2}} W dW \quad (11)$$

These results enable one to define a very useful quantity depending only on the nuclear matrix elements, known as the ft value of the transition:

$$ft = 5.57 \times 10^{-20} g^{-2} [|f_1|^2 + K^2 |f_0|^2] \text{ sec.} \quad (12)$$

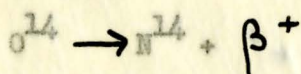
Where g is expressed in units of $mc^2 (h/mc)^3 = 4.73 \times 10^{-38} \text{ erg cm}^3$.

Thus any two decays can in principle serve to determine g and K^2 . However, the matrix elements f_0 can be calculated exactly only for the neutron, in which case:

$$\begin{aligned} |f_0|^2 &= 3 \\ \text{and} \\ |f_1|^2 &= 1 \end{aligned}$$

$|f_1|^2$ can be calculated exactly for several other nuclei as well as long as one may assume the charge-independence of nuclear forces.

The most recent value of g is that due to Gerhardt (8) who investigated the decay:



This is a $0 \rightarrow 0$ (no) transition so that $f_0 = 0$ and g may be calculated directly. The value he obtained was:

$$g = 1.374 \pm 0.016 \times 10^{-49} \text{ erg cm}^3$$

Combining this with the data on the neutron decay he found:

$$K^2 = 1.37 \pm \begin{matrix} 0.40 \\ 0.30 \end{matrix}$$

Finkelstein and Moskowski (9) have listed some other fairly

reliable values of K^2 based on Gerhardt's value of g :

$H^3 \rightarrow He^3$	1.82	\pm	0.1
$O^{15} \rightarrow N^{15}$	1.97	\pm	0.4
$F^{17} \rightarrow O^{17}$	1.30	\pm	0.15

A direct determination of K^2 has been made by Robson (28) who measured the angular correlations between electron and proton in the decay of the neutron. His result was:

$$K^2 = 1.49 \begin{array}{l} + 1.44 \\ - 0.56 \end{array}$$

Of course, simple calculations of this type can only yield the value of K^2 . That is why a determination of the sign of K necessitates the rather lengthy analysis of forbidden spectra described below.

Chapter 11. The Theory of Forbidden Spectra and the Method of Conies.

Empirically, the various degrees of forbidden-ness of beta-transitions may be roughly identified by their ft values. Konopinski and Langer (5) for instance, give the following classifications:

<u>Type</u>		<u>$\log_{10} ft$</u>
allowed	{favoured	2.0 - 3.7
	{normal	4.0 - 5.8
first forbidden	{unique	7.3 - 10.1
	{normal	6.0 - 8.0
second forbidden		12.2 - 13.5

"Favoured" transitions all have $\Delta K \leq 3$ and are either between mirror isobars or members of isobaric triads. "Unique" first forbidden transitions are those with $\Delta J = 2$, (yes) so that only the tensor matrix elements contribute to the decay (see below).

This classification corresponds quite well with that based on the spin and parity changes predicted by the theory. There are however, several exceptions that can only be explained by postulating additional selection rules; these are discussed in detail in the review articles of Preston (3) and Konopinski and Langer (5).

In order to simplify the exposition of the theory it is convenient to neglect Coulomb effects so that the wave-functions of both electron and neutrino may be taken as plane-waves:

$$\psi = A e^{i \mathbf{p} \cdot \mathbf{r}}; \quad \phi = B e^{-i \mathbf{q} \cdot \mathbf{r}}$$

A, B are, of course, 4-element column vectors.

Since the de Broglie wave lengths of the electron and the neutrino are, in general, large compared to nuclear dimensions, we can evaluate the matrix elements of Chapter 1 in successive approximations, corresponding to an expansion of ψ and ϕ in successive powers of $(p + q \cdot r)$. For example in the scalar interaction we can put $\beta = 1$ and write:

$$(\psi * \phi) = A^*B \left[1 - i (p + q \cdot r) - \frac{1}{2} (p + q \cdot r)^2 \dots \dots \right] \quad (13)$$

The first term corresponds to an allowed transition with the selection rules given in Chapter 1. Higher terms in the expansion correspond to forbidden transitions whose selection rules are given by Konopinski and Uhlenbeck (13). For the interactions of current interest a slightly simplified version of their result is:

<u>Interaction</u>	<u>First Forbidden</u>	<u>Second Forbidden</u>
Scalar	0, ± 1 (no $0 \rightarrow 0$) Yes	$\pm 1, \pm 2$ (no $1 \leftrightarrow 0$) No
Tensor	0, $\pm 1, \pm 2$ Yes	$0 \rightarrow 0, \pm 2, \pm 3$ No
Pseudoscalar	0, ± 1 (no $0 \rightarrow 0$) No	$\pm 1, \pm 2$, (no $1 \leftrightarrow 0$) Yes

The spectrum shape of forbidden transitions can be conveniently expressed in the form of Equation 9 multiplied by a "correction factor" C_n for an n-forbidden transition. It is clear from Equation 13 that C_n will be a function of p and q so that the Fermi plot of $\left[\frac{N}{p^2 F} \right]^{\frac{1}{2}}$ against W (where N is the number of electrons with momentum between p and p + dp) will in general not be a straight line. In order to obtain a straight

line it is necessary to plot $[N/p^2FC]^{1/2}$ against W .

In the rigorous derivation of the correction factor ψ must be a solution of the Dirac equation in a Coulomb field. The difficulty then arises that the result contains the radial wave-functions of the electron which are singular at the origin. However, this is without physical significance since the Coulomb field undoubtedly breaks down within the nucleus. This difficulty is avoided by calculating the radial wave-functions at a value of r which has the order of magnitude of the nuclear radius.

The correction factors for single interactions have been given by Konopinski and Uhlenbeck (13), and Greuling (14). The cross-terms that occur with mixed interactions have been worked out by Pursey (15).

Morita et al (10) investigated the spectra of Fe^{59} , Rb^{87} , Tc^{99} , and Cs^{137} and found that their Fermi plots could all be linearised only if K were negative. Owing to the neglect of certain corrections their analysis is not accurate for each particular case; the authors claim that their conclusion is deduced from a "rather statistical" standpoint.

Similarly, consideration of the shapes of $\Delta J=2$, (no) spectra, led Peaslee (11) to the conclusion that K is negative. On the other hand, Lee-Whiting (12) analysed the spectrum of Bi^{120} by a method very similar to that described in Chapter 11 and found that K should be positive. However, he did not work out the various parameters involved to the degree of accuracy found necessary in the calculations described in Chapter 11.

By comparing the theoretical correction factor with the experimental results it is possible in principle to determine the relative sign of the scalar and tensor interactions directly. However, because of the large

cancellation that occurs between the terms of the correction factor it is more accurate to use an indirect method that involves the drawing of conics. This method was originally devised by Lee-Whiting (12) and has been considerably refined by M. A. Preston, J. M. Pearson and the present writer.

The Method of Conics.

Assuming that the interaction consists only of the scalar and tensor terms, the correction factor for second-forbidden transitions is given by:

$$G = G_{2s} + G_{2t} + G_{2st} \quad (14)$$

Where the terms arise from the scalar, the tensor and the cross-product interactions respectively.

In Pursey's notations the correction factor for an electron of momentum p is:

$$\begin{aligned} G(p) = & \epsilon_s^2 \left| Q_2(\beta \underline{E}) \right|^2 F(p) + \epsilon_t^2 \left| Q_2(\beta \underline{\sigma} \times \underline{E}) \right|^2 f(p) \\ & + \epsilon_t^2 \left| Q_2(\beta \underline{\alpha}) \right|^2 h(p) + \epsilon_t^2 \left| Q_3(\beta \underline{\sigma}) \right|^2 k(p) \\ & + \epsilon_t^2 \left[Q_2(\beta \underline{\sigma} \times \underline{E}) Q_2^*(\beta \underline{\alpha}) + c.c. \right] g(p) \\ & - \epsilon_s \epsilon_t i \left[Q_2(\beta \underline{E}) Q_2^*(\beta \underline{\alpha}) - c.c. \right] H(p) \\ & - \epsilon_s \epsilon_t i \left[Q_2(\beta \underline{E}) Q_2^*(\beta \underline{\sigma} \times \underline{E}) - c.c. \right] G(p) \end{aligned} \quad (15)$$

Where $F(p)$, $f(p)$ etc., are certain functions of momentum and symbols like $Q_2(\beta \underline{E})$ represent certain nuclear matrix elements that are defined below.

We now introduce the quantities:

$$x = \frac{i g_t Q_2 (\beta \sigma x \underline{I})}{g_s Q_2 (\beta \underline{I})} \quad (16)$$

$$y = \frac{i g_t Q_2 (\beta \underline{I})}{g_s Q_2 (\beta \underline{I})}$$

which have been shown to be real by Longuire and Messiah (16).

Substituting x and y in Equation 15 we obtain:

$$\frac{C(p)}{g_s^2 |Q_2(\beta \underline{I})|^2} = F(p) + f(p) x^2 + h(p) y^2 + 2g(p) xy + 2H(p)y + 2G(p)x + k(p) \frac{g_t^2 |Q_3(\beta \sigma)|^2}{g_s^2 |Q_2(\beta \underline{I})|^2} \quad (17)$$

The last term is small and will be neglected in the first instance although it will be taken into account in Chapter III.

If the correction factor at some other momentum p_0 is $C(p_0)$ then:

$$\rho = \frac{C(p)}{C(p_0)} = \frac{f(p) x^2 + h(p) y^2 + 2g(p) xy + 2H(p)y + 2G(p)x + F(p)}{f(p_0) x^2 + h(p_0) y^2 + 2g(p_0) xy + 2H(p_0)y + 2G(p_0)x + F(p_0)} \quad (18)$$

Therefore:

$$\left[f(p) - \rho f(p_0) \right] x^2 + \left[h(p) - \rho h(p_0) \right] y^2 + \dots = 0 \quad (19)$$

i.e. $f' x^2 + 2g' xy + h' y^2 + 2G' x + 2H' y + F' = 0 \quad (20)$

This is the equation of a conic, and the intersection of two or more such conics gives the values of x and y that fit the experimental results. Then g_t/g_s can be calculated if either of the ratio of the matrix elements that occur in Equation 16 are known.

In practice, the experimental Fermi-plot is corrected to an arbitrary straight line of slope m (say). The equation of this line is:

$$\left[\frac{N}{Cp^2 F} \right]^{\frac{1}{2}} = m (W_0 - W)$$

i.e.

$$C(p) = \frac{N}{p^2 F m^2 (W_0 - W)^2}$$

Therefore, $\rho = C(p)/C(p_0)$ is independent of the slope of the straight line.

It remains to define the symbols that occur in Equation 15. The usual system of relativistic units will be used, i.e., the unit of mass is the electron mass m , the unit of length is \hbar/mc , the unit of time is \hbar/mc^2 , the unit of energy is mc^2 and the unit of momentum is mc .

The functions of $F(p)$, $f(p)$, etc., can be written in terms of the neutrino momentum q as:

$$F(p) = \frac{1}{30} L_0 q^4 + \frac{2}{15} N_0 q^3 + \frac{1}{3} M_0 q^2 + \frac{2}{3} L_1 q^2 + 2N_1 q + 3M_1 + 4.5L_2$$

$$f(p) = \frac{1}{45} L_0 q^4 - \frac{2}{15} N_0 q^3 + \frac{1}{3} M_0 q^2 + \frac{1}{3} L_1 q^2 - 2N_1 q + 3M_1 + 2L_2$$

$$h(p) = \frac{1}{3} L_0 q^2 + 3L_1$$

$$g(p) = \frac{1}{15} L_0 q^3 + \frac{1}{3} N_0 q^2 - L_1 q + 3N_1$$

$$k(p) = \frac{1}{30} L_0 q^4 + L_1 q^2 + 7.5L_2$$

$$H(p) = \frac{1}{15} L_0 q^3 - \frac{1}{3} N_0 q^2 - L_1 q - 3N_1$$

$$G(p) = \frac{1}{3} L_1 q^2 - \frac{1}{3} M_0 q^2 + 3L_2 - 3M_1$$

The functions of L_n , M_n and N_n are infinite series in terms of the effective nuclear radius R . The first three terms of the series were found sufficient in each case:

$$L_n = \frac{F_n}{F_0} \left[\frac{2^n n!}{(2n+1)!} p^n \right]^2 \times [{}^0L_n + {}^1L_n + {}^2L_n + \dots]$$

$${}^0L_n = \frac{n+1+S_n}{2n+2}$$

$${}^1L_n = \frac{-1}{2S_n+1} \left[\frac{S_n}{(n+1)^2} \frac{1}{W} + \frac{2n+3+2S_n}{n+1} W \right] \alpha Z R$$

$${}^2L_n = \frac{1}{(2S_n+1)^2 (n+1)} \left[\frac{1}{n+1} + \frac{4S_n+3}{S_n+1} \left\{ n+2+S_n + \frac{S_n}{n+1} \right\} \right]$$

$$+ p^2 \left\{ 2 \frac{1}{(n+1+S_n)} + \frac{(n+2+S_n)(4S_n+3)}{S_n+1} - \frac{2S_n+1}{2(n+1-S_n)} \right\} (\alpha Z R)^2$$

$$M_n = \frac{F_n}{F_0} \left[\frac{2^{n+1} n!}{(2n+2)!} p^n \right]^2 \times [{}^{-2}M_n + {}^{-1}M_n + {}^0M_n + \dots]$$

$${}^{-2}M_n = \frac{n+1}{2(n+1+S_n)} \left(\frac{\alpha Z}{R} \right)^2$$

$${}^{-1}M_n = \left\{ \frac{S_n}{2S_n+1} \frac{p^2}{W} - \frac{(2n+1)(\alpha Z)^2}{(2S_n+1)(n+1+S_n)} W \right\} \frac{\alpha Z}{R}$$

$${}^0M_n = \frac{(n+1)(S_n-n) S_n}{(2S_n+1)^2} \left[1 - \frac{(4S_n+3)(\alpha Z)^2}{S_n(S_n+1)} \right] p^2$$

$$+ \left[1 + \frac{n(4S_n+3)(\alpha Z)^2}{(S_n+1)(n+1+S_n)} \right] \left(\frac{\alpha Z}{(2S_n+1)} \right)^2$$

$$N_n = \frac{-F_n}{F_0} \left[\frac{(2^n n! p^n)}{(2n+1)!} \right]_{n+1}^2 \times \left[\begin{array}{l} -^1N_n + \circ N_n + ^1N_n \\ + \dots \dots \dots \end{array} \right]$$

$$-^1N_n = \frac{1}{2} \left(\frac{\alpha Z}{R} \right)$$

$$\circ N_n = \frac{S_n \frac{p^2}{W} - 2(\alpha Z)^2 W}{2S_n + 1}$$

$$^1N_n = \left[\frac{(\alpha Z)^2 (4S_n + 3) + [(\alpha Z)^2 (4S_n + 3) - (5S_n + 5S_n^2 + 1)] p^2}{(S_n + 1) (2S_n + 1)^2} \right] (\alpha Z R)$$

In these formulae S_n is defined by:

$$S_n = \left[(n+1)^2 - (\alpha Z)^2 \right]^{\frac{1}{2}}$$

and

$\frac{F_n}{F_0}$ is given by:

$$\frac{F_n}{F_0} = \frac{1}{2} \left[\frac{(2n+2)!}{n!} \right]^2 (2pR)^2 (S_n - S_0 - n) \frac{|\Gamma(S_n + it)|^2 [\Gamma(1 + 2S_0)]^2}{|\Gamma(S_0 + it)|^2 [\Gamma(1 + 2S_n)]^2}$$

t is defined by:

$$t = \alpha Z \frac{W}{p}$$

The electron and neutrino momentum p , q are related to the electron energy W and the end-point energy W_0 by:

$$W^2 = p^2 + 1$$

$$q = W_0 - W$$

The author is greatly indebted to Mr. J. M. Pearson (17) who worked out some of the higher terms in the expansions of L , M and N .

Symbols like $Q_2 (\beta \underline{\mathbf{r}})$ represent nuclear matrix elements that are second-rank tensors of the form:

$$Q_2(\underline{\mathbf{a}}) = \frac{1}{2} \int U_f^* \left[a_i x_j - \frac{1}{3} \delta_{ij} (\underline{\mathbf{a}} \cdot \underline{\mathbf{r}}) \right] U_i dV$$

Where the x_j are the components of the position vector $\underline{\mathbf{r}}$.

Similarly $Q_3 (\beta \underline{\mathbf{r}})$ represents a third-rank tensor of the form:

$$Q_3(\underline{\mathbf{a}}) = \frac{1}{6} \int U_f^* \left[a_i x_j x_k - \frac{1}{5} \delta_{ij} a_k r^2 - \frac{2}{5} \delta_{ij} x_k (\underline{\mathbf{a}} \cdot \underline{\mathbf{r}}) \right] U_i dV$$

These expressions are to be summed over the indices i, j, k .

Chapter 111. Construction and Analysis of the Conics.

In order to pick a suitable forbidden decay for investigation it is necessary to consider whether the ratios of matrix elements in Equation 6 can be calculated. Such calculations can only be carried out with the aid of some nuclear model. The shell model allows some particularly simple calculations but should be used only when it may be reasonably reliable. It seems that the assignment of the shell for an even mass nucleus is more difficult than for an odd mass nucleus where there is just one nucleon outside the core so that investigations are usually restricted to odd mass nuclei. In this case first-forbidden transitions can supply no information since they all show the allowed shape spectrum. The suitable cases are apparently confined to the second-forbidden transitions of Fe^{59} , Te^{99} and Cs^{137} , and the third-forbidden transition of Rb^{87} . The work described below is an investigation of the spectrum of Cs^{137} .

The decay scheme of Cs^{137} is shown in Figure 1. According to the single particle shell model, the transition to the ground state of the nucleon is $g_{7/2} \rightarrow d_{3/2}$ (no) so that it is second-forbidden for both scalar and tensor interactions. The calculated ratio of the matrix elements involved in π is (10) :

$$Q_2 \frac{(\beta \underline{\sigma} \times \underline{r})}{Q_2(\beta \underline{I})} = -1 \quad (21)$$

so that:

$$\pi = \frac{g_t}{g_s} \quad (22)$$

The ratio of matrix elements involved in γ cannot be readily calculated but fortunately it is not needed.

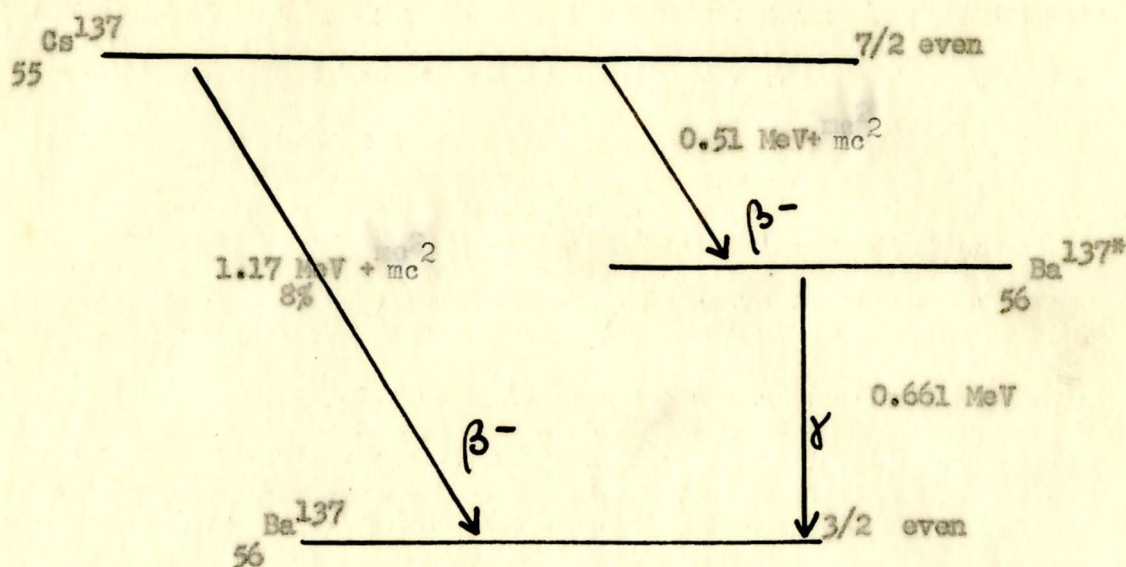


Fig. 1.
Decay Scheme of Cs^{137} .

Because of the transition to the excited state, only the high-energy portion of the second-forbidden spectrum can be determined.

The experimental results used were those of Langer and Moffat (18) who kindly made their original data available (19). From this data the Fermi-plots shown in Figure 2, were drawn with the help of the tables of the Fermi-function $F_0(Z,W)$ issued by the National Bureau of Standards (20). The three curves represent three separate sets of experimental results obtained with different source-strengths and spectrometric transmissions. Screenings corrections were found to be smaller than the experimental error and were therefore neglected. The spectrum was corrected to the straight line shown; the correction factors being evaluated at the four momentum values $p = 2.2, 2.4, 2.6$ and 2.8 . The reference momentum F_0 was taken to be 2.4 since this seemed on the most reliable portion of the curves. The value of ρ was calculated for each curve and the mean value taken.

It was rather difficult to estimate the probably errors of the ρ values obtained in this way. However, inspection revealed that the curves could be drawn to fit the experimental points with an uncertainty of about $2\frac{1}{2}\%$. This implies an uncertainty of 5% in $G(p)$ and an uncertainty of 10% in ρ . It was therefore decided to use three values of ρ , including the mean value and values differing from it by $\pm 7\%$.

These results are given in Table 1, at the end of this chapter.

A preliminary calculation was carried out using the values of L, M and N listed in the tables of Rose et al (21) where they are given to only four figures. With the accuracy obtainable in this way it was found that the centres of the conics could not be precisely determined and the criterion for reality of the conics (described below) could not be applied because of the large amount of cancellation that occurred. It was concluded that L, M and N should be known to an accuracy of at least five figures so that it was necessary to calculate them from the formulae found in Chapter 11.

This procedure also made it possible to take account of different possible values of effective nuclear radius and the end-point energy.

The effective nuclear radius R_e is the value of r at which the radial electron wave-functions are evaluated. Since the electron can be produced anywhere in the nucleus R_e could presumably be considerably smaller than the total nuclear radius R_0 . R_e was taken to be $\frac{1}{2} \propto A^{1/3}$ where A is the atomic number; this value is a little larger than that which is currently used in most work. The calculation was carried through for $R_e/R_0 = 0.5, 0.6, 0.7, 0.8, 0.9$ and 1.0 , but conics were drawn only for ratios of $0.5, 0.8$ and 1.0 .

The end-point energy is given by Langer and Moffat (18) as $W = 3.29 \text{ mc}^2$; presumably the estimated error is 0.005 mc^2 . Therefore three values of W_0 were used in the calculation, i.e.,

$$W_0^- = 3.285 \text{ mc}^2, W_0^0 = 3.290 \text{ mc}^2, W_0^+ = 3.295 \text{ mc}^2$$

The value of the fine structure constant used in the calculations was that recently given by Cohen et al. (22) :

$$\alpha = 7.29729 \pm 0.00003 \times 10^{-3}$$

Although the calculation and the construction of the conics were found to be quite straightforward in general, there are several important considerations which are perhaps not quite obvious. These are dealt with in the following sections.

Calculation of the Complex Gamma Function.

The functions of $\Gamma(S_n + it)$ were calculated from the National Bureau of Standards tables (23) with the aid of tables of Lagrangian interpolation coefficient (24).

The tables list the values of U, V of the real and imaginary parts of the logarithm of the gamma function, which makes it easy to calculate the modulus.

i.e.

Let $\Gamma(S_n + it) = R e^{i\theta}$

Then: $|\Gamma(S_n + it)|^2 = R^2$

but: $\log \Gamma(S_n + it) = \log R + i\theta = U + iV$

Therefore: $U = \log R$

Therefore:

$$2U = \log (R)^2 = \log |\Gamma(s_n + it)|^2$$

Therefore:

$$|\Gamma(s_n + it)|^2 = \text{Antilog } 2U$$

It was found that 5 point interpolation was sufficient to calculate $\log \Gamma(z)$ to seven decimal places so long as $|z| \geq 3$. Therefore for $|z| \sim 1$ i.e., $n = 0$, it was necessary to calculate $\log \Gamma(z+2)$ and for $|z| \sim 2$ i.e., $n = 1$, it was necessary to calculate $\log \Gamma(z+1)$.

In the first case we have:

$$\Gamma(z) = \frac{\Gamma(z+2)}{z(z+1)}$$

i.e.

$$|\Gamma(z)|^2 = \frac{|\Gamma(z+2)|^2}{|z(z+1)|^2}$$

and since $z = s_0 + it$

$$|\Gamma(z)|^2 = [(s_0^2 + t^2)^2 + (s_0^2 + t^2)(1 + 2s_0)]^{-1} |\Gamma(z+2)|^2$$

Similarly we obtain:

$$|\Gamma(z)|^2 = [s_1^2 + t^2]^{-1} |\Gamma(z+1)|^2$$

The gamma functions of real argument were easily calculated by 5-point interpolation from the tables of Davies (25).

Determination of the Nature of the Conics.

It was shown in Chapter 11 that the Equation of the conics is:

$$f'x^2 + 2g'xy + h'y^2 + 2G'x + 2H'y + F' = 0$$

It is not sufficient simply to plot these curves, since it is very important to know whether the conic is real, which class it belongs to and what the co-ordinates of its centre are.

These properties are determined by the following "auxiliary coefficients" :

$$\delta = g'^2 - f'h'$$

$$\epsilon = h'g' - H'g'$$

$$\eta = g'g' - H'f'$$

$$\Delta = G'\epsilon - H'\eta + F'\delta$$

$$A = h'F' - H'^2$$

$$B = f'F' - G'^2$$

The nature of the conic is then determined as follows (26) :

<u>Class I</u>	<u>The Parabolic Curves</u>	<u>$\delta = 0$</u>
$\Delta \neq 0$	a parabola	
$\Delta = 0$	(I) $A + B > 0$ (II) $A + B = 0$ (III) $A + B < 0$	equation inconsistent straight line two parallel lines
<u>Class II</u>	<u>The Elliptical Curves</u>	<u>$\delta < 0$</u>
$\Delta = 0$	a point ellipse	
$\Delta / (f' + h') < 0$	equation inconsistent	
$\Delta / (f' + h') > 0$	a proper ellipse	
<u>Class III</u>	<u>The Hyperbolic Curves</u>	<u>$\delta > 0$</u>
$\Delta = 0$	intersecting line pair	
$\Delta \neq 0$	a hyperbola	

The co-ordinates of the centre are given by:

$$X = \epsilon / \delta, \quad Y = -\eta / \delta$$

The Effect of the Extra Matrix Element.

In chapter 11 we neglected the small term:

$$K = k(p) \frac{\epsilon_t^2}{\epsilon_s^2} \frac{|Q_3(\beta\sigma)|^2}{|Q_2(\beta\pi)|^2} \sim k(p) \frac{|Q_3(\beta\sigma)|^2}{|Q_2(\beta\pi)|^2}$$

This term is independent of x or y so that if we take it into account we merely find that:

F' becomes $F' + K'$
i.e. Δ becomes $\Delta + K'\delta(\epsilon, \gamma)$ and δ are unaltered so that the centre remains unchanged).

In the case of an ellipse the effect is to decrease Δ so that the ellipse shrinks towards a point at its centre. In the case of a hyperbola the effect is to increase Δ so that when Δ is positive as is usually the case, the curve shrinks away from its asymptotes. In both cases the effect is to widen the bands but always towards the interior of the curves drawn for $K = 0$.

The Accuracy of the Calculation.

The preliminary calculation indicated that f, g , etc., must be known to at least five figures since otherwise the terms in Δ all cancel out. This requires that L, M, N and the q 's be known to at least five figures.

L, M and N can only just be calculated to five figures because the fine structure constant is known to only five figures and this is therefore the maximum accuracy obtainable in calculating terms like $R^2 (S_n - S_{0-n})$

that occur in F_N/F_0 (see Chapter 11). Therefore it was legitimate to take only the first three terms in the expansions of L, M and N since it was found that the fourth term only affects the sixth figure.

q can be calculated to sufficient accuracy only if we make $W_0 = 3.290000$ and then vary its value from $W_0 - = 3.285000$ to $W_0 + = 3.295000$.

The Effect of Finite Nuclear Size.

The wave-function of the electron near the nucleus is altered if one takes account of the fact that the electron is not actually moving in the field of a point charge but in the field of a finite charge distribution.

A correction to the values of L, M and N which takes account of this fact has been introduced by Rose (27). Of course, such a correction can be only approximate since the exact charge distribution in the nucleus is not known.

For $Z = 56$ the corrections are quite small, never greater than a few percent, but even such small changes might be very important when L, M and N have to be calculated to five figures.

In this calculation these corrections were not made. There were two reasons for this. Firstly, because of the approximations involved in calculating the correction there would still be a large uncertainty in the corrected values, so that it is questionable whether the very considerable extra labour involved would be worth while. Secondly, it is felt that these corrections would be largely covered by the variation in effective nuclear radius that was allowed for in the calculation. This is because a change

in the value of r at which the electron wave-function is computed has much the same effect as a change in the wave-function itself. Moreover, the variation in L , M and N that is caused by the change in effective nuclear radius is far greater than that caused by the effect of finite nuclear size. The magnitude of both effects is greatest for M , followed by N and L .

Results.

The numerical values of L , M and N are given in Table 2 at the end of this chapter, Table 3 gives the values of F , f , h , g , k , H and G , and Table 4 gives the values of the auxiliary coefficients δ , ϵ , γ and Δ .

The results in Tables 2 and 3 are given to six figures but the last figure is not reliable as explained above. The auxiliary coefficients are worked out to as many figures as possible assuming five figure accuracy in F , f , etc., The effects of heavy cancellation especially in Δ are obvious.

The conics drawn from these results are shown in Figures 3, 4 and 5. Generally they are bands due to the uncertainty in end-point energy and experimental correction factors. There are, of course, three sets of bands corresponding to $p = 2.2$, 2.6 , and 2.8 . However, the bands are generally so narrow and the overlapping so complete that it is not possible to reproduce them separately in black and white. Consequently it is just the envelope of all the bands that is shown except in the case of $R_e/R_0 = 1.0$ where the band for $p = 2.2$ can be distinguished from the other two.

The manuscript containing the details of the entire calculation and the original conics remain in the hands of Dr. M. A. Preston at McMaster University.

Discussion of the Results.

Reference to Table 4 will show that in some cases the curves are real only for one value of the experimental correction factors used. This means that the band thickness used corresponds only to the variation in end-point energy. Before becoming imaginary the curves shrink to a point whose position can be roughly estimated from the variation of the auxiliary coefficients. This point is always in the interior of the curves drawn, so that the effect of taking account of the entire range of permissible ρ values would be merely to widen the bands towards the interior.

In some cases the curves are hyperbolae but since $x = g_t/\epsilon_s$ must certainly be less than 2, the branches in the positive quadrant can always be neglected. Some considerations pertinent to Figures 3, 4 and 5 individually are given below:

Figure 3. $R_e/R_o = 1.0$

Some of the curves for $p = 2.8$ are hyperbolae. However, their centre is approximately at $x = 8$ so that the positive branches may be neglected.

Figure 4. $R_e/R_o = 0.8$

All the real curves are hyperbolae. The centres are at $x = 3$ or 4 so that the positive branches may be neglected.

Two of the curves for $p = 2.8$, $\rho = 0.265$ should be intersecting line pairs since $\Delta = 0$, but in fact they turn out to be hyperbolae when plotted. This is not so surprising as the calculation of Δ involves 3rd order cancellations whereas the actual plotting of the conic involves only 2nd order cancellations. It is important to note that the calculation of

the co-ordinates of the centre involves only 2nd order cancellation and is therefore quite reliable. The remaining curve in this band is a parabola, but calculation of the auxiliary coefficients A and B showed that it is imaginary.

Figure 5. $R_0/R_0 = 0.5$

Most of the curves are hyperbolae with centres at $x = 1.3$ to 2 , so that again the positive branches may be neglected. For $p = 2.6$ there are some very small ellipses around $x = 0.6$.

It appears that the effect of taking smaller effective nuclear radii is that the centres of the conics approach the origin while the slope of the principal axis becomes greater. It is therefore possible that for R_0/R_0 less than 0.5 the hyperbolae in the positive quadrant would come so close to the origin that positive values of x of reasonable absolute magnitude would become possible.

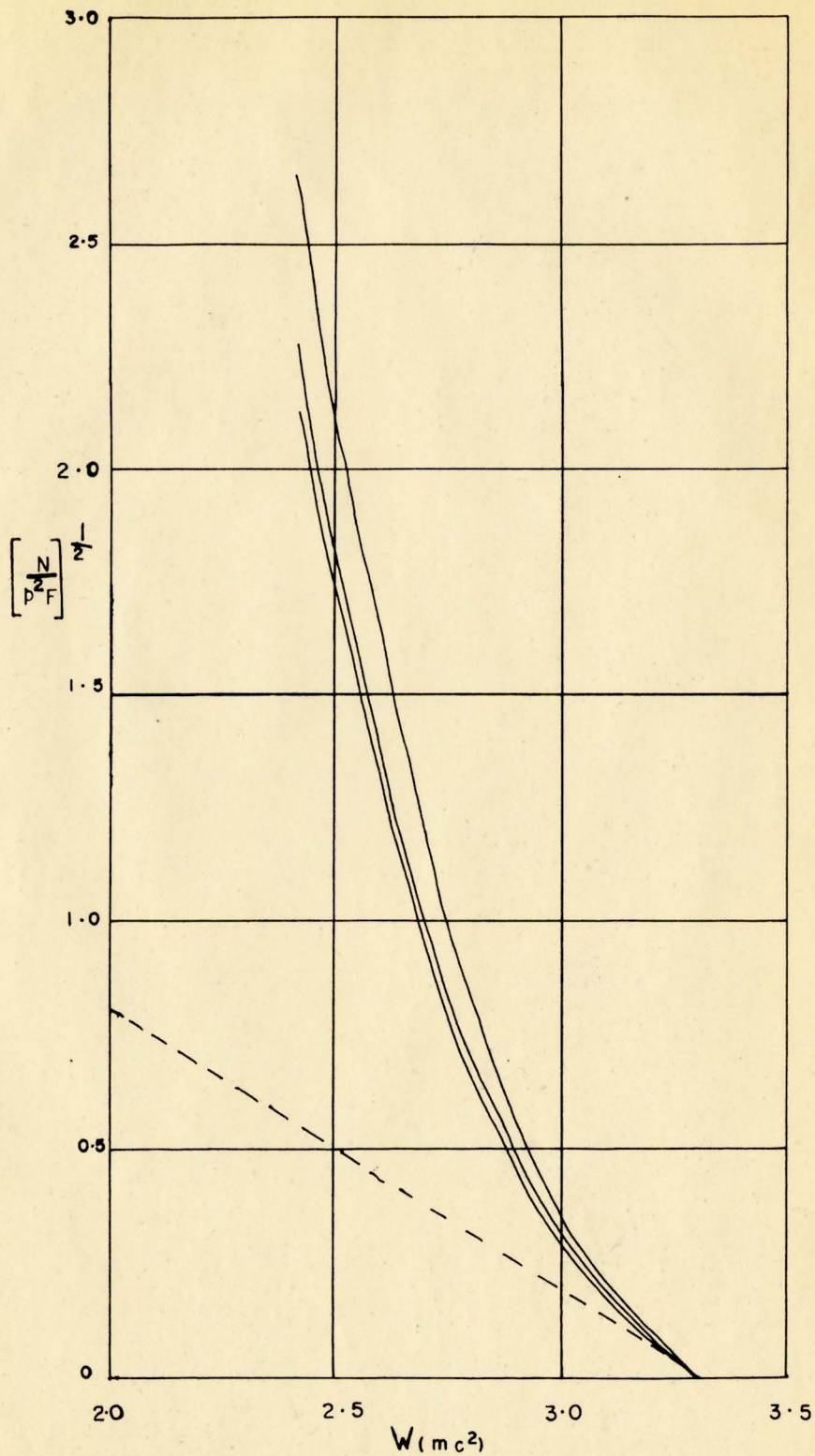
The results are consistent with those obtained by Morita et al (10) who found that the Cs^{137} spectrum could be fitted with values of E_1/E_2 of -1 or -2 but not with values of $+1$ or $+2$. They defined a quantity \wedge proportional to our y/x . The ratio of their values of \wedge for $x = -1$ and $x = -2$ is:

$$\frac{\wedge(x = -1)}{\wedge(x = -2)} = 1.32 \text{ or } 1.34$$

This is in perfect agreement with the corresponding ratio of the two values of y/x which is 1.32 and 1.34 for the lower and upper branches respectively of the conics for $R_0/R_0 = 1$.

As a final check a particular combination of values of x and y

i.e., $(-1, -11.4)$ was taken from the conics for $R_e/R_o = 1$ and substituted in Equation 17. The correction factor obtained in this way gave a good straight line when applied to the experimental Fermi plot.



W (mc²)
Fig. 2.

Fermi-plot of the second-forbidden transition of Cs¹³⁷.

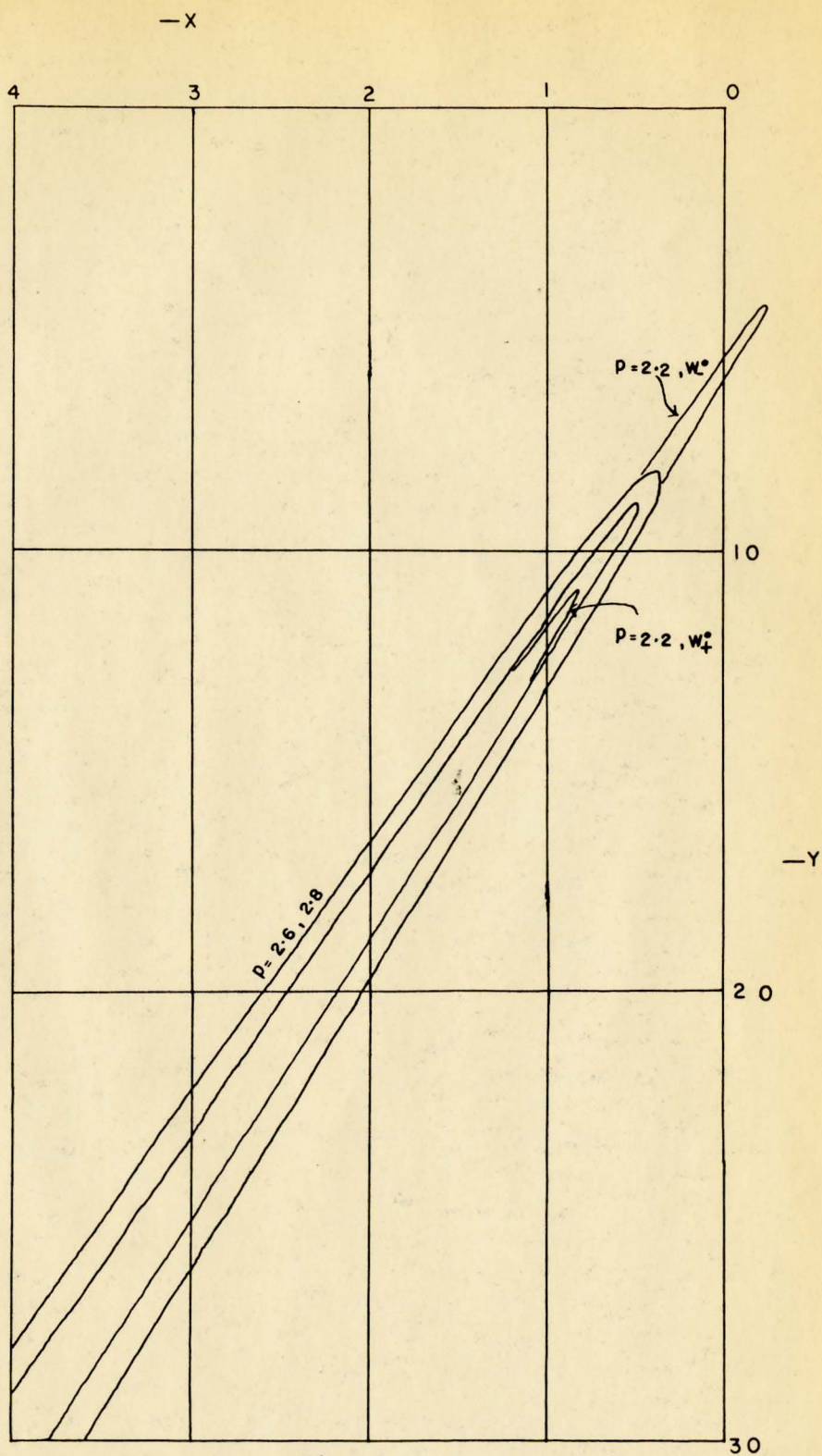


Fig. 3.
 Conic envelopes for $R_e/R_0 = 1.0$
 (30a)

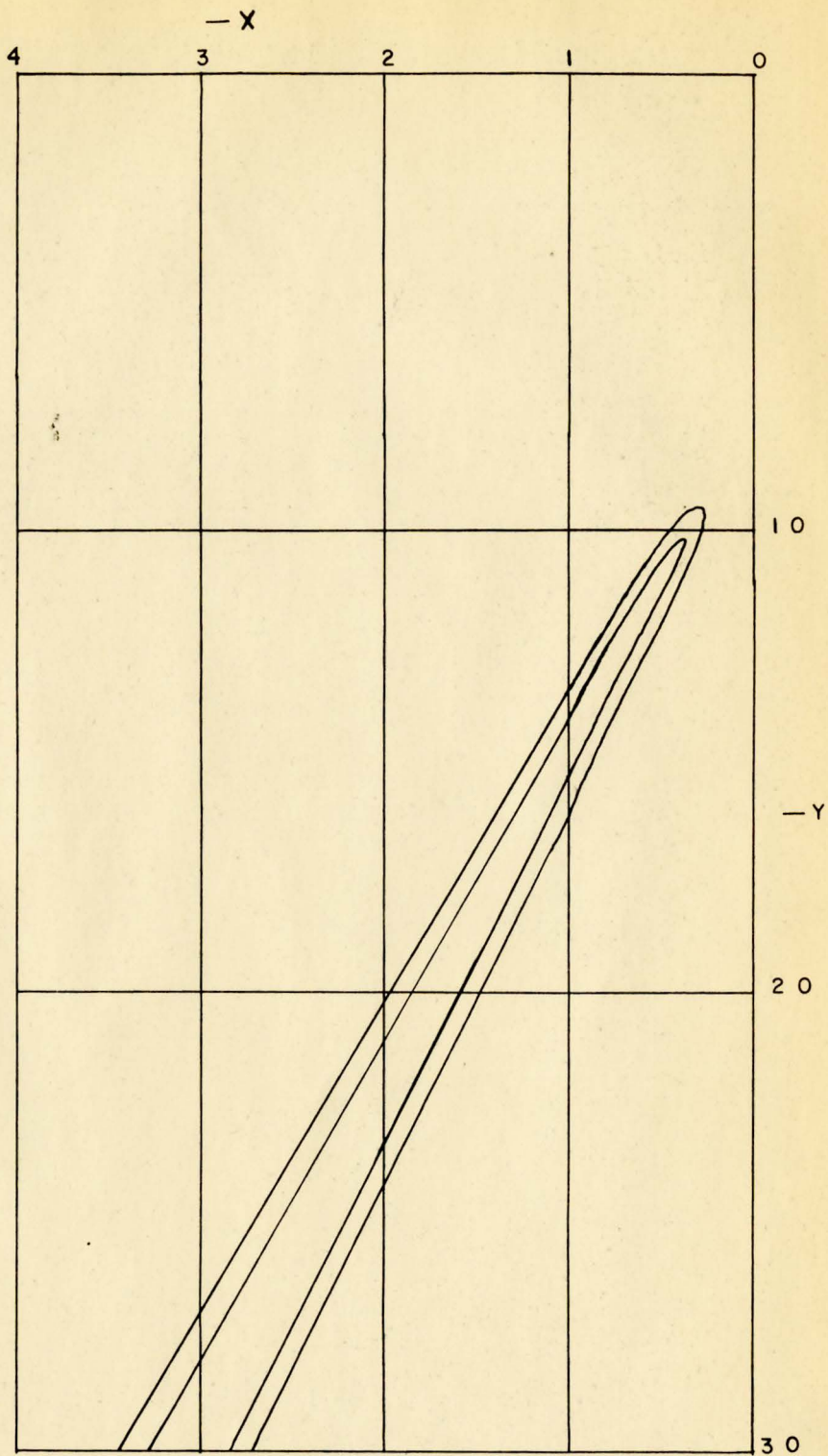


Fig. 4.
 Conic envelopes for $R_e/R_0 = 0.8$
 (30b)

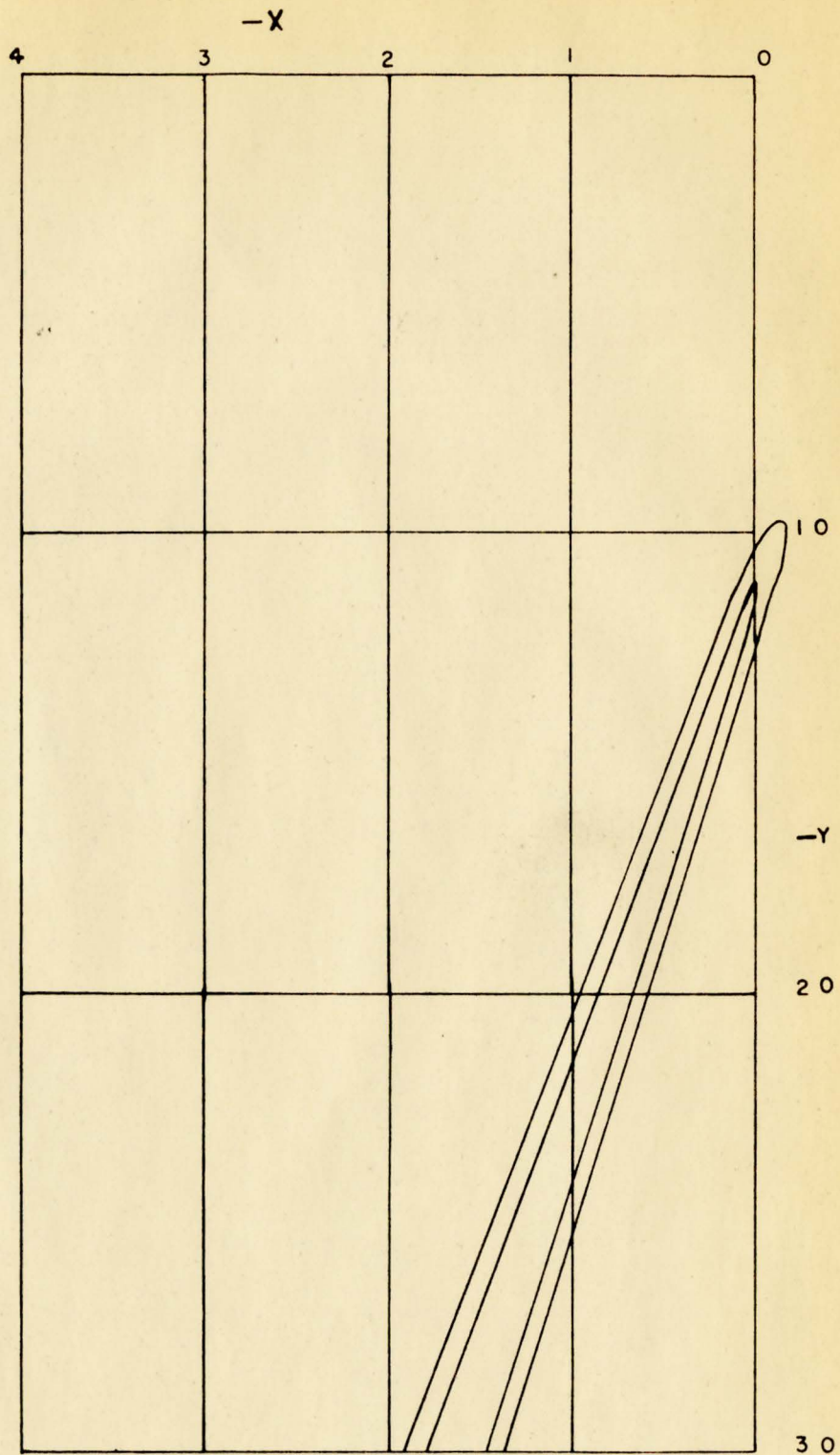


Fig. 5.
Conic envelopes for $R_e/R_0 = 0.5$

(30c)

Table 1.
Values of Experimental Correction Factor.

P	C(P)			P(P)			Mean P(P)
2.2	15.33	17.43	23.96	1.687	1.700	1.631	1.67 [±] 0.12
2.4	9.088	10.25	14.69				
2.6	4.802	5.454	7.925	0.5284	0.5321	0.5395	0.536 [±] 0.036
2.8	2.567	2.991	4.140	0.2825	0.2918	0.2818	0.285 [±] 0.020

Table 2.
Values of L, M and N.

R_e/R_o :	0.5	0.8	1.0
<u>p=2.2</u>			
L ₀	0.939945	0.930080	0.923493
L ₁	0.401572	0.416736	0.423684
L ₂	0.0710079	0.0748105	0.0766312
<u>p=2.4</u>			
L ₀	0.938768	0.928187	0.921119
L ₁	0.478741	0.496617	0.504756
L ₂	0.100876	0.106248	0.108813
<u>p=2.6</u>			
L ₀	0.937570	0.926261	0.918703
L ₁	0.563151	0.583936	0.593336
L ₂	0.139460	0.146846	0.150361
<u>p=2.8</u>			
L ₀	0.936356	0.924307	0.916251
L ₁	0.654840	0.678721	0.689447
L ₂	0.188352	0.198269	0.202976

$R_e/R_o :$		0.5	0.8	1.0
<u>p=2.2</u>	M_0	518.637	208.546	136.030
	M_1	52.1541	22.0894	14.7935
	M_2	4.06708	1.75283	1.18449
<u>p=2.4</u>	M_0	521.409	210.291	137.433
	M_1	62.6528	26.6403	17.8863
	M_2	5.824489	2.52122	1.70843
<u>p=2.6</u>	M_0	524.163	212.026	138.829
	M_1	74.2597	31.6977	21.3342
	M_2	8.11784	3.52854	2.39745
<u>p=2.8</u>	M_0	526.902	213.753	140.219
	M_1	87.0011	37.2772	25.1501
	M_2	11.0513	4.82357	3.28598

$R_e/R_o :$	0.5	0.8	1.0
<u>$p=2.2$</u>	N_0 -22.0771	-13.9237	-11.2039
	N_1 -4.57578	-3.03230	-2.50223
	N_2 -0.537317	-0.361983	-0.301104
<u>$p=2.4$</u>	N_0 -22.1221	-13.9675	-11.2469
	N_1 -5.47596	-3.63604	-3.00308
	N_2 -0.766424	-0.517364	-0.430902
<u>$p=2.6$</u>	N_0 -22.1662	-14.0103	-11.2888
	N_1 -6.46587	-4.30071	-3.55589
	N_2 -1.06384	-0.719542	-0.600037
<u>$p=2.8$</u>	N_0 -22.2096	-14.0523	-11.3299
	N_1 -7.54683	-5.02812	-4.16171
	N_2 -1.44252	-0.977542	-0.816175

Table 3.

Values of F , f etc. Three values are given corresponding to end-point energies W_0^0 , W_0^- and W_0^+ respectively.

$p=2.2$

R_e/R_0 :	0.5	0.8	1.0
$F(p)$:	278.925 277.496 280.362	113.328 112.772 113.888	74.1311 73.8254 74.5388
$f(p)$:	298.547 296.960 300.142	126.097 125.438 126.758	84.6081 84.1696 85.0489
$h(p)$:	1.44372 1.44099 1.44646	1.48670 1.48400 1.48942	1.50587 1.50319 1.50857
$g(p)$:	-19.7334 -19.6666 -19.8006	-13.0426 -12.9994 -13.0860	-10.7666 -10.7312 -10.8021
$k(p)$:	0.857114 0.853203 0.861053	0.897010 0.892971 0.901077	0.915837 0.911741 0.919962
$H(p)$:	18.9484 18.8871 19.0101	12.2320 12.1944 12.2699	9.94446 9.91475 9.97433
$G(p)$:	-288.021 -286.517 -289.534	-118.965 -118.361 -119.573	-78.6314 -78.2377 -79.0272

p = 2.4

$R_0/R_0 :$	0.5	0.8	1.0
F(p):	262.793 261.671 263.923	106.307 107.872 106.745	71.4895 71.2126 71.7684
f(p):	279.514 278.242 280.795	119.220 118.687 119.756	80.4087 80.0518 80.7681
h(p):	1.58521 1.58305 1.58737	1.63715 1.63503 1.63930	1.66045 1.65834 1.66258
g(p):	-20.2895 -20.2360 -20.3434	-13.4878 -13.4528 -13.5229	-11.1626 -11.1338 -11.1915
k(p):	0.991592 0.988097 0.995115	1.04031 1.03670 1.04396	1.06337 1.05970 1.06707
H(p):	19.5878 19.5399 19.6360	12.7618 12.7327 12.7911	10.4257 10.4028 10.4487
G(p):	-270.328 -269.134 -271.530	-112.897 -112.416 -113.381	-75.0630 -74.7492 -75.3790

p = 2.6

$R_0/R_0:$	0.5	0.8	1.0
F(p):	261.058 260.239 261.853	109.253 108.946 109.563	72.7721 72.5790 72.9674
f(p):	274.447 273.493 275.409	117.991 117.585 118.400	79.9046 79.6300 80.1815
h(p):	1.76894 1.76737 1.77052	1.83034 1.82879 1.83190	1.85790 1.85636 1.85945
g(p):	-21.5689 -21.5288 -21.6094	-14.3923 -14.3657 -14.4192	-11.9318 -11.9097 -11.9541
k(p):	1.19120 1.18830 1.19414	1.25186 1.24835 1.25490	1.28060 1.27754 1.28368
H(p):	20.9848 20.9508 21.0192	13.7875 13.7643 13.8080	11.3176 11.3020 11.3335
G(p):	-266.752 -265.876 -267.637	-112.579 -112.225 -112.936	-75.2712 -75.0399 -75.5047

p = 2.8

$R_0/R_0:$	0.5	0.8	1.0
F(p):	274.645 274.171 275.127	116.674 116.502 116.850	78.4158 78.3113 78.5226
f(p):	283.903 283.271 284.545	122.646 122.369 122.928	83.2549 83.0633 83.4437
h(p):	1.99584 1.99486 1.99634	2.06708 2.06611 2.06807	2.09899 2.09803 2.09997
g(p):	-23.5929 -23.5662 -23.6199	-15.7714 -15.7532 -15.7898	-13.0845 -13.0691 -13.1001
k(p):	1.47867 1.47659 1.48078	1.55544 1.55329 1.55763	1.59182 1.58963 1.59404
H(p):	23.1740 23.1541 23.1943	15.3375 15.3262 15.3489	12.6438 12.6354 12.6523
G(p):	-278.041 -277.490 -278.602	-118.365 -118.141 -118.591	-79.5083 -79.3626 -79.6573

Table 4.

Values of the auxiliary coefficients. Three values are given corresponding to end-point energies of W_0^0 , W_0^- and W_0^+ respectively.

$p = 2.2$

$R_e/R_0 = 0.5$

ρ :	1.55	1.67	1.79
δ	+ 0.74, +0.84, +0.66	-2.27, -2.09, -2.40	-6.18, -5.96, -6.41
ϵ	+ 0.96, +1.07, +0.87	-1.96, -1.78, -2.09	-5.75, -5.53, -5.98
γ	- 2.8, -2.9, -2.7	-3.0, -3.0, -3.0	-3.0, -3.1, -3.0
Δ	0, -1, 0 Real	+2, +2, +1 Imaginary	+9, +8, +6 Imaginary

$R_e/R_0 = 0.8$

ρ :	1.55	1.67	1.79
δ	+0.153, +0.189, +0.112	-1.145, -1.086, -1.215	-2.82, -2.74, -2.93
ϵ	+0.483, +0.522, +0.441	-0.680, -0.618, -0.750	-2.21, -2.12, -2.31
γ	-2.52, -2.55, -2.50	-3.16, -3.21, -3.15	-3.78, -3.85, -3.72
Δ	-0.2, -0.3, -0.2 Real	+1.3, +1.2, +1.4 Imaginary	+3, +3, +4 Imaginary

$R_e/R_0 = 1.0$

ρ :	1.55	1.67	1.79
δ	-0.027, -0.002, -0.055	-0.928, -0.884, -0.969	-2.080, -2.018, -2.143
ϵ	+0.347, +0.373, +0.320	-0.406, -0.361, -0.448	-1.392, -1.328, -1.456
γ	-2.28, -2.29, -2.28	-2.94, -2.97, -2.92	-3.62, -3.66, -3.59
Δ	-0.1, -0.1, -0.1 Real	+1.0, +1.0, +1.1 Imaginary	+2.7, +2.6, +2.9 Imaginary

$$p = 2.6$$

$$R_e/R_o = 0.5$$

ρ :	0.500	0.536	0.572
δ	-0.99, -0.91, -1.05	-0.21, -0.16, -0.27	+0.494, +0.532, 0.450
ϵ	-0.63, -0.55, -0.70	+0.11, +0.16, +0.04	+0.777, +0.819, +0.729
η	-4.0, -4.0, -3.9	-3.7, -3.8, -3.6	-3.4, -3.4, -3.3
Δ	0 0 0 point	+1, +2, +1 real	+1, 0, 0 real

$$R_e/R_o = 0.8$$

ρ :	0.500	0.536	0.572
δ	-0.572, -0.540, -0.596	-0.232, -0.207, -0.254	+0.073, +0.092, +0.056
ϵ	-0.144, -0.135, -0.170	+0.151, +0.156, +0.128	+0.412, +0.412, +0.394
η	-3.10, -2.93, -3.07	-2.83, -2.68, -2.81	-2.54, -2.41, -2.54
Δ	-0.5, -0.4, -0.4 Imaginary	-0.1, -0.2, -0.2 Imaginary	0, +0.1, +0.2 Real

$$R_e/R_o = 1.0$$

ρ :	0.500	0.536	0.572
δ	-0.471, -0.450, -0.491	-0.238, -0.221, -0.253	-0.028, -0.015, -0.040
ϵ	-0.017, +0.006, -0.038	+0.170, +0.187, +0.153	+0.334, +0.348, +0.321
η	-2.69, -2.71, -2.68	-2.46, -2.45, -2.44	-2.21, -2.21, -2.20
Δ	-0.4, -0.3, -0.4 Imaginary	-0.1, -0.1, -0.1 Imaginary	+0.1, +0.1, +0.1 Real

p = 2.8

R_e/R₀ = 0.5

P	:	0.265	0.285	0.305
δ				
ε		+1.17, +1.28, +1.09	+1.83, +1.94, +1.76	+2.50, +2.56, +2.41
γ		+2.33, +2.43, +2.24	+2.93, +3.04, +2.87	+3.56, +3.63, +3.45
		-13.6, -13.6, -13.4	-13.0, -13.0, -13.0	-12.5, -12.7, -12.4
Δ		+4, +6, +2	+6, +6, +3	+5, +7, +7
		Real	Real	Real

R_e/R₀ = 0.8

P	:	0.265	0.285	0.305
δ				
ε		+0.06, +0.10, 0	+0.34, +0.38, +0.31	+0.64, +0.66, +0.58
γ		+1.38, +1.41, +1.32	+1.60, +1.64, +1.57	+1.85, +1.88, +1.80
		-9.8, -9.8, -9.8	-9.4, -9.4, -9.4	-9.05, -9.13, -9.15
Δ		0 0 0	0 0 0	+2, +1, +3
		Real Imag.	Real	Real

R_e/R₀ = 1.0

P	:	0.265	0.285	0.305
δ				
ε		-0.23, -0.19, -0.26	-0.024, +0.002, -0.047	+0.167, +0.193, +0.147
γ		+1.15, +1.186, +1.12	+1.304, +1.331, +1.281	+1.445, +1.472, +1.424
		-8.42, -8.37, -8.40	-8.08, -8.09, -8.09	-7.79, -7.80, -7.78
Δ		0, +1, +1	+0.9, +1.0, +1.1	+1.4, +1.4, +1.2
		Real	Real	Real

Conclusions.

It is quite impossible to draw any conclusions about the absolute magnitude of g_t/g_s since there is complete overlapping of the conics. It is clear that such overlapping would occur no matter how accurately the experimental spectrum was determined, since in some cases the band thickness corresponds only to the uncertainty in end-point energy. As explained above, the effect of taking account of the extra matrix element and of the entire range of permissible ρ values would be to widen the bands towards the interior.

It was explained in Chapter III that two assumptions are necessary before any conclusions can be drawn from this work: Firstly, that the effect of the finite nuclear size is allowed for by taking different effective nuclear radii and secondly, that the effective radius should not be smaller than half the total radius.

On this basis, the analysis enables one to draw a definite conclusion about the sign of g_t/g_s . Since the absolute value of x cannot be greater than two, the conics for all three radii show that x must be negative. Therefore g_t/g_s is negative.

References.

1. H.A.Bethe and R.F.Bacher, Rev. Mod. Phys. 8, 82, (1936.)
2. E.J.Konopinski, Rev. Mod. Phys. 15, 209, (1943).
3. M.A.Preston, Nat. Res. Coun. Canada Report LT-29, (1950)
4. T.H.R.Skyrme, Progress in Nuclear Physics (Academic Press Inc.)
1, 115, (1950)
5. E.J.Konopinski and L.M.Langer, Annual Reviews of Nuclear Science
(Annual Reviews Inc.) V.2, 261, (1953)
6. W.Pauli, Handbuch der Physik, 24, 301 et seq.
7. C.S.Wu, Proc. Glasgow Conference on Nuclear Physics, (Pergamon
Press) 177, (1954)
8. J.B.Gerhardt, Phys. Rev. 95, 288, (1954)
9. R.J.Finkelstein and S.A.Mozkowski, Phys. Rev. 95, 1695, (1954)
10. M.Morita, J.Fujita, and M.Yamada, Progr. Theor. Phys. 10, 630, (1953)
11. D.C.Pearlee, Phys.Rev. 91, 1447, (1953)
12. G.E.Lee-Whiting, Phys.Rev. 97, 463, (1955)
13. E.J.Konopinski and G.E.Uhlenbeck, Phys. Rev. 60, 308, (1941)
14. E.Greuling, Phys.Rev. 61, 568, (1942)
15. D.L.Pursey, Phil. Mag. 42, 1193, (1951)
16. C.L.Longmire and A.M.L.Messiah, Phys.Rev. 83, 464, (1951)
17. J.M.Pearson, Personal Communication.
18. L.M.Langer and R.J.D.Moffat, Phys. Rev. 82, 635, (1951)
19. L.M.Langer, Personal Communication.
20. Tables for the Analysis of Beta Spectra, Nat. Bur. Stands., Applied
Mathematics Series, 13, (1952)

References - (continued) -

21. M.E.Rose, C.L.Perry, and N.M.Dismuke, Tables for the analysis of allowed and forbidden beta-transitions. O.R.N.L. Report 1459. (1953)
22. E.R.Cohen, J.W.M.DuMond, T.W.Layton and J.S.Rollett, Rev. Mod. Phys., 27, 363, (1955)
23. Tables of the Gamma Function for Complex Arguments, Natl. Bur. Stands. Applied Mathematics Series, 34, (1954)
24. Tables of Lagrangian Interpolation Coefficients, Nat. Bur. Stands, Columbia Univ. Press, New York, (1944)
25. H.T.Davies, Tables of the Higher Mathematical Functions, Principia Press, Bloomington, Indiana (1933)
26. F.D.Murnaghan, Analytic Geometry, Prentice Hall, New York, (1946)
27. M.E.Rose and D.K.Holmes, Phys. Rev. 83, 190, (1951)
28. J.M.Robson, Phys. Rev. 100, 933, (1955)